Dominance of climate warming effects on recent drying trends over wet monsoon regions

Chang-Eui Park[1,2], Su-Jong Jeong[1], Chang-Hoi Ho[2], Hoonyoung Park[2], Shilong Piao[3], Jinwon Kim[4], Song Feng[5]

[1]School of Environmental Science and Engineering, South University of Science and Technology of China, Shenzhen, 518055, China
[2]School of Earth and Environmental Sciences, Seoul National University, Seoul, 08826, South Korea
[3]College of Urban and Environmental Sciences, Peking University, Beijing, 100871, China
[4]Department of Atmospheric and Oceanic Sciences, University of California, Los Angeles, 90024, CA, USA
[5]Department of Geosciences, University of Arkansas, Fayetteville, 72701, AR, USA

Aug 2017
Atmospheric Chemistry and Physics

Correspondence to: Su-Jong Jeong (waterbell@gmail.com)

Abstract

Understanding changes in background dryness over the land is key information for adapting to climate change because of the critical socioeconomic consequences. However, causes of continental dryness changes remain uncertain because various climate parameters control dryness. Here, we verify dominant climate variables determining dryness trends over continental East Asia, which is characterized by diverse hydro-climate regimes ranging from arid to humid, by quantifying the relative effects of changes in precipitation, solar radiation, wind speed, surface air temperature, and relative humidity on trends in aridity index based on observed data from 189 weather stations for the period of 1961-2010. Before the early 1980s (1961-1983), change in precipitation is a primary condition for determining aridity trends. In the later period (1984-2010), dominant climate parameter on aridity trends varies according to the hydro-climate regime. Drying trends in arid regions are mostly explained by reduced precipitation. In contrast, the increase in potential evapotranspiration due to increased atmospheric water-holding capacity, a secondary impact of warming, works to increase aridity over the humid monsoon region despite enhanced water supply and relatively less warming. Our results show significant drying effects of the warming over the humid monsoon region in recent decades; this also supports the drying trends over the warm and water-sufficient regions in future climate.

1 Introduction

The background dryness over the land varies as climate changes, but major climate parameter driving dryness changes remains unclear in many regions (Sherwood and Fu, 2014; Hegerl et al., 2015). In previous assessments, precipitation (*P*), the amount of water supply, is regarded as a key variable for understanding variations in dryness, particularly in humid regions such as Asian monsoon regions (Wang et al., 2012; Kitoh et al., 2013; Liu and Allan, 2013). For example, in East Asia, dryness changes are generally summarized as "the dry northwestern region (west of 100°E and north of 30°N) is getting wetter, the dry northern region (east of 100°E and north of 35°N) is getting drier, and the wet southeastern region (east of 100°E and south of 35°N) is getting wetter" based on changes in annual mean *P* (Wang and Ding, 2006; Piao et al., 2010). In addition, a decrease in *P* leads to drying trends over the northern and central-east regions of India, part of the South Asian monsoon region (Zhou et al., 2008; Roxy et al., 2015). However, climate change also varies potential evapotranspiration (*PET*), the amount of atmospheric moisture demand (Liu et al., 2010; Han et al., 2012; Shan et al., 2012). *PET* variations largely affect dryness trends that are in turn closely related to the occurrence of droughts, water scarcity, and tree mortality (Westerling et al., 2006; Park Williams et al., 2013; Dai, 2013). Drying impacts of *PET* increase are usually emphasized in water-limited regions (Westerling et al., 2006; Estes et al., 2014); however, humid areas are also expected to experience severe aridification in the 21st century because of a continuous increase in *PET* (Feng and Fu, 2013; Cook et al., 2014). Thus, the processes involved in the variability of dryness need to be examined over various hydro-climate regimes to better understand continental dryness changes.

This study aims to elucidate the mechanisms of dryness trends in continental East Asia through the analysis of observed climate data at 179 and 10 weather stations in mainland China and South Korea, respectively, for the period 1961−2010. The long-term trend in dryness is a critical concern for continental East Asia, as it is a region of massive populations, widely varying hydro-climate regimes, fragile ecosystems, and significant agricultural activities (Piao et al., 2010; Geng et al., 2014; Jeong et al., 2014). Also, the analysis region has recently experienced abrupt climate changes (Gong and Ho 2002; Yue et al., 2013). For example, northeast China experienced severe warming by 0.36 ºC decade^{-1} for the period of 1960-2006 (Piao et al. 2010). Rainfall intensity has significantly increased over southeastern China (Zhai et al., 2005). Further, changes in the hydrological cycle over East Asia is not consistent with a well-known paradigm "dry regions drier, wet regions wetter" in spite of significant warming trend (Greve et al., 2014).

Previous assessments on trends in surface dryness show contradictory results over continental East Asia. Assessments based on grid reanalysis data generally suggest that continental East Asia is getting drier due to an increase in *PET* accompanied by an increase in the vapor pressure deficit (VPD) (Feng and Fu, 2013; Greve et al., 2014; Huang et al., 2016). On the contrary, the other studies using site observations reported that more than half of the stations over mainland China show negative trends in both *PET/P* and *PET*, indicating a decrease in surface dryness, following a decrease in solar irradiance and wind speed despite continuous warming (Wu et al., 2006; Zhang et al., 2009; Huang et al., 2016). Thus, a quantitative analysis is needed to explain the contradiction between previous assessments regarding surface dryness over continental East Asia.

In this study, an aridity index, *PET/P*, defined as *PET* based on the Penman–Monteith method (Allen et al., 1998) divided by *P*, is employed to assess surface dryness and its trends (Middleton et al., 1997; Estes et al., 2014; Greve et al., 2014). Over the land surface, the amount of actual evaporation (*AET*) is constrained by the amount of *P*, which is also generally less than *PET* because of limited available water at the surface (Fu and Feng, 2014; Greve et al., 2014). Thus, the *PET/P* ratio is more suitable for measuring the degree of water deficiency or surplus for a certain climate condition. If the value of *PET/P* is less than unity, the location is classified as a wet region, and vice versa. Likewise, as the aridity index decreases, the land surface becomes wetter, and vice versa. By the definition of the aridity index, trends in surface dryness can be resolved by combining the effects of changes in five climate parameters: *P*, net radiation (*Rn*), wind speed (*WS*), surface air temperature (*Ta*), and relative humidity (*RH*). Furthermore, we classify the analysis domain into three hydro-climate regimes based on the 50-year climatology of *PET/P*: arid ($PET/P \geq 2$), transitional ($1 \leq PET/P < 2$), and humid ($PET/P < 1$) (Geng et al., 2014) (Fig. 1). The ratio *PET/P* and regional classification allow the identification of climate parameters that are important for trends in surface dryness over the three hydro-climate regimes.

2 Methods and data

To compute the aridity index, *PET/P*, climate data for the period 1961−2010 are obtained from 179 and 10 meteorological sites in mainland China and South Korea, respectively. Quality of these data is controlled by the National Meteorological

Center of the China Meteorological Administration and Korea Meteorological Administration. Data include daily precipitation, daily mean air temperature, 10-m wind speed, relative humidity, and sunshine duration. The last four variables are used to compute daily *PET* following the Penman-Monteith method (Allen et al., 1998; see section 1 in supplementary information for details). We computed the daily *PET* and *PET/P*, and then estimated their annual-mean values at individual weather sites. Due to the decadal variation of East Asian monsoon circulation (Ding et al., 2008; Ha et al., 2012), the entire analysis period is divided into two sub-periods, 1961-1983 and 1984-2010, by applying three change-point methods to the temporal variations of *PET/P* (Pettitt, 1980; Lund and Reeves, 2002; Beaulieu et al., 2012, see section 2 of supplementary information for details). The data at each meteorological sites satisfy the following criteria: 1) all climate parameters in the year 2010 exist, 2) sufficient records for at least 10 years for the two sub-periods (i.e., 1961–1983 and 1984–2010).

To identify the climate variables that contribute most to the observed *PET/P* trends, relative influences of changes in *P*, *Rn*, *WS*, *Ta*, and *RH* on the *PET/P* trends are computed at individual weather sites based on the derivative of *PET/P* with respect to time as following:

$$\frac{d}{dt}\left(\frac{PET}{P}\right) = -\frac{PET}{P^2}\frac{dP}{dt} + \frac{1}{P}\frac{dPET}{dt} \qquad (1)$$

The first and second terms on right-hand side indicate temporal changes in the aridity index due to the changes in *P* and *PET*. *PET* can be decomposed into *Rn*, *WS*, *Ta*, and *RH* four climate parameters using multilinear regression (Chattopadhyay and Hulme, 1997; Yin et al., 2010; Dinpashoh et al., 2011; Han et al., 2012; see section 3 in supplementary information for details). Then, the equation (1) is written as follows:

$$\frac{d}{dt}\left(\frac{PET}{P}\right) \approx -\frac{\overline{PET}}{\bar{P}^2}\frac{dP}{dt} + \frac{1}{\bar{P}}\left(a_{Rn}\frac{dR_n}{dt} + a_{WS}\frac{dWS}{dt} + a_{Ta}\frac{dT_a}{dt} + a_{RH}\frac{dRH}{dt}\right) \qquad (2)$$

where the terms on the right-hand side are the trend in *PET/P* considering changes in *P*, *Rn*, *WS*, *Ta*, and *RH*, indicate the relative effects of *P*, *Rn*, *WS*, *Ta*, and *RH*, respectively. $\bar{P}$ and $\overline{PET}$ are the average of the annual-mean *P* and *PET* for the analysis period, respectively.

3 Results

3.1 Trends in *PET/P*, *P*, and *PET* over continental East Asia

Figure 2 shows climatology of annual-mean *PET/P*, *P*, and *PET* of all analysis stations over continental East Asia for the period of 1961-2010. *PET/P* is significantly varied by regions: getting larger to northwestern direction and smaller to southeastern direction (Fig 2a). This spatial pattern of *PET/P* is caused by both northwest-southeast patterns of *P* and small regional variation of *PET* (Figs. 2b and 2c). The annual-mean *PET/P* is decreased over most of analysis domain (86.7% of total weather stations) during 1961-2010 by both increase in *P* and decrease in *PET* (Fig. 3). Note that the scale of the *P* trends (Fig. 3b) is reversed in order to represent drying and wetting trends as red and blue colors, respectively. The negative trends in *PET/P* are large and significant at 95% confidence level over the northwestern China (< 100ºE), whereas the eastern part of the analysis domain (> 100ºE), classified by monsoon climate zone, shows small and insignificant trends in *PET/P* (Fig. 3a). The spatial pattern of the trends in *P* is similar to that of *PET/P* with opposite sign (Figs. 3a and 3b). At more than half of the sites, the trends in *PET* is significant, but the magnitude of *PET* trends is small (Fig. 3c).

The wetting trends over the arid northwestern China are caused by significant increase in *P* rather than the decrease in *PET* (Fig. 3), also consistent with previous assessments (Zhai et al., 2005; Shi et al., 2007; Piao et al., 2010). However, over monsoon climate regions, more detailed analysis is needed due to the decadal variation in large-scale atmospheric circulation and rainfall (Ding et al., 2008; Piao et al., 2010). Figure 4 depicts the temporal variation in the mean *PET/P* for the arid, transitional, and humid regimes over monsoon regions (> 100ºE) expressed as annual mean anomalies. Note that the temporal variations are the averages of *PET/P* anomalies at 56, 50, and 51 weather sites located on arid, transitional, and humid climate regimes, respectively. For all three climate regimes, the *PET/P* anomalies show abrupt changes in early 1980s (see section 2 of supplementary information for details). Also, the trends in *PET/P* anomalies are not significant in the arid and humid regimes. Thus, the analysis of *PET/P* changes over the monsoon regions needs a separation of the analysis period.

The spatial distributions of *PET/P* trends show considerable changes between both analysis periods (Figs. 5a and 5d). For the earlier period, about 60% of the total number of stations show decreasing trends in *PET/P*, particularly in the arid (northwestern and northern China) and humid regions (southeastern China) (Fig. 5a). Increasing trends in *PET/P*, with relatively small magnitudes, occur mainly in the transitional region (northeastern and southwestern China). The spatial pattern of the *P* trend is similar to that of the *PET/P* trend but with the opposite sign, suggesting that the changes in *P* are directly linked to changes in *PET/P* for most of the analysis region (Figs. 5a and 5b). Decreasing trends in *PET* appear in more than three-quarters of the analysis domain, but these are significant only in humid regions because of their small magnitudes (Figs. 5a and 5c).

In the later period, the spatial patterns of the *PET/P*, *P*, and *PET* trends change drastically over the monsoon climate regions (Figs. 5d–5f). The trends in *PET/P* shift from negative to positive values in both the humid (southeastern China) and arid (northern and northeastern China) regions (Figs. 5a and 5d). These notable alterations of the *PET/P* trend are explained by changes in *P* and *PET* trends. After the early 1980s, positive trends of *P* are reversed in the arid regions, and the magnitude of the increasing trends in *P* decreases in the humid regions (Figs. 5b and 5e). These changes in *P* trends are consistent with those in *PET/P* trends over the arid regions but not in the humid area (Figs. 5d and 5e). Significant increases in *PET* leads to the positive trends in *PET/P* in the humid area despite the increase in *P* (Figs. 5d–5f).

The different spatial patterns of *PET/P* trends between both analysis periods are consistent with regional patterns of changes in climate variables over East Asian monsoon regions. The variations of *P* are directly associated with the decadal variability of the East Asian monsoon circulation. As monsoon circulation weakened, both meridional circulation and southerlies in lower atmosphere decreased over the East Asian monsoon region; hence, moisture transport is concentrated over southern China (Ding et al., 2008). These changes create favorable conditions for rainfall over the southern China (humid monsoon region) but opposite situations over the northern China (arid monsoon region). Since the late 1970s, weakening of monsoon circulation has led to significant decreases and increases in *P* over arid and humid monsoon regions, respectively (Ding et al., 2008; Piao et al. 2010). The increasing trend in *P* over the humid area decreases or reverses as a result of the reduction in monsoon rainfall related to the recovery of monsoon circulation after the early 1990s (Liu et al., 2012; Zhu et al., 2012). As a consequence of changes in the monsoon circulation, the decreasing trends in *P* in the arid region are greater than the increasing trends in the humid area (Fig. 5e). Changes in other climate fields are linked to the positive *PET* trends (Fig. 5f). For example, the warming trend becomes more severe in the later period (Ge et al., 2013; Yue et al., 2013) (Figs. S3c and S3g). The trend in absorbed solar radiation changed from dimming to brightening, particularly in the humid region (Tang et al., 2011) (Figs. S3a and S3e). Consequently, the combined impacts of changes in climate parameters resulted in the increase in *PET/P* for 1984-2010.

3.2 Relative influences of five climate parameters on changes in dryness trends

Figure 6 shows spatial distribution of the relative influences of five climate variables over the continental East Asia for 1961-1983 and 1984-2010. Here, positive values of a particular variable indicate increasing rates of *PET/P* with respect to changes in that variable only, and vice versa. Overall, *PET/P* trends are strongly affected by changes in *P* in both analysis periods. Influences of other four variables are generally small, but in part comparable to those of *P*. In the early period, changes in *P* decrease *PET/P* in the arid (northwestern China and Inner Mongolia) and humid regions (southeastern China), also increase *PET/P* over a part of the transitional (Shandong Peninsula) and arid (Bohai Bay) (Fig. 6a). Changes in *PET/P* due to other climate parameters are negligible except relatively large influences of *Rn* over the humid regions (Figs. 6b-6e). In the later period, *P* shows positive influences over the northeastern China (arid and transitional regions are co-existed), but reduces *PET/P* over the arid (northwestern China) and humid regions (southeastern China) (Fig. 6f). Relative influences of *Rn* shows similar magnitudes to that of *P* over the transitional area (Shandong Peninsula) (Figs. 6f and 6g). Over the humid regions (southeastern China), positive influences of *RH* are on a par with the negative influences of *P* (Figs. 6f and 6j).

The spatial patterns of relative effects of climate parameters are significantly different according to the analysis periods and regions, indicating that the mechanisms involved in changing *PET/P* trends operate differently. Figure 7 displays the averaged effects of five climate parameters over the three hydro-climate regimes for the two analysis periods. The confidence intervals are computed at the 95% significance level based on relative influences of five variables at 56, 50, and 51 stations of arid, transitional, and humid climate regimes (see section 3 in supplementary information for details). Note that this analysis focuses on the monsoon region, which shows significant variability in the trends of *PET/P*. Stations located in western China (west of 100°E) are excluded. The mean climate of western China is distinctly different from the monsoon climate (Piao et al., 2010). Furthermore, the dryness trends in these regions are more strongly associated with variations in *P* for both analysis periods than with other climate variables (Fig. 6, and Zhai et al., 2005; Shi et al., 2007).

Over the arid region, the positive effects of *P*, *Ta*, and *RH* (1.15%, 0.44%, and 0.55% decade^{-1}, respectively) increase the *PET/P* before the early 1980s (Fig. 7a). Large confidence range of *P* indicates a substantial impact of *P* on the *PET/P* trends locally (Fig. 6a). In the later period, the change in *P* provides the largest influence (3.27% decade^{-1}), at least twice the magnitude of any other climate parameter. These results imply that the decrease in *P* is the main cause of the significantly increasing trend in *PET/P* over the arid region. In the transitional region, the negative influence of *Rn* (-0.85% decade^{-1}) appears to be the largest in the earlier period (Fig. 7b), but the wide confidence interval of *P* suggests that *PET/P* trends vary spatially according to the changes in *P* (Fig. 6a). In the later period, *PET/P* increased because of the positive influences of changes in *P*, *Ta*, and *RH* (2.02%, 0.97%, and 0.99% decade^{-1}, respectively), despite the negative effects of *Rn* and *WS* (-0.34% and -0.48% decade^{-1}, respectively). Thus, the increasing trend of *PET/P* in the transitional region is largely a consequence of surface warming (i.e., *Ta*) and decreases in *P* and *RH*. Over the humid area, negative effects of both *P* and *Rn* (-4.52% and -2.06% decade^{-1}, respectively) lead to the decrease of *PET/P* in the earlier period (Fig. 7c). The contribution from each of the other three variables is much smaller. In contrast, in the later period, the positive influences of *Ta* and *RH* (0.79% and 1.81% decade^{-1}, respectively) are somewhat larger than the negative influences of *P* and *Rn* (-1.08% and -0.70% decade^{-1}, respectively). Thus, the increasing trend in *PET/P* over the humid region is mainly caused by the warming and subsequent increase in atmospheric water demand.

4 Discussions and Conclusions

The present study suggests that trends in surface dryness reverse from wetting to drying around the early 1980s over both arid and humid monsoon regions. In addition, major climate parameters determining dryness trends vary by both the analysis period and hydro-climate regime. For the period of 1961-1983, trends in surface dryness are mostly attributed to changes in *P*, regardless of region. A significant decrease in *Rn* reinforces wetting trends over the humid area by decreasing *PET*. Large influences of *P* and *Rn* on dryness trends are consistent with the results of previous studies on trends in aridity and *PET* using daily observations of weather (Wu et al., 2006; Han et al., 2012).

In the later period, changes in *P*, *Ta*, and *RH* lead to drying trends over the monsoon regions. Figure 8 illustrates the impacts of the three variables on the dryness trend in the arid and humid monsoon regions, respectively. Over the arid monsoon region, *PET/P* is greatly increased by the positive effects of the three variables, whereas the humid monsoon region shows relatively small increases in *PET/P* because the positive effects of *Ta* and *RH* are offset by the negative effects of *P*. In contrast to the importance of the effect of evaporative potential on surface dryness in other water-limited regions (Westerling et al., 2006; Estes et al., 2012), the decrease in *P* plays a dominant role in the increasing *PET/P* trends in the arid monsoon region. In the humid monsoon area, the decrease in *RH* shows the largest effect on the *PET/P* trend, despite the relatively small magnitude of warming. The relationship between air temperature and saturation vapor pressure (e_s) (e.g., the Clausius–Clapeyron equation) explains the large influence of the decrease in *RH*. Due to high mean temperatures in the humid monsoon region (shades of the map in Fig. 8), warming leads to a steep increase in e_s, and a subsequent decrease in *RH*, resulting in a large increase in evapotranspiration.

Our results based on point observations already include various anthropogenic impacts such as land use/land cover changes (LULCC) and increased aerosol emissions, which can influence climate and further surface dryness (Menon et al., 2002; Guo et al., 2013). For example, in the later period, positive influences of *P* are generally inconsistent with negative influences of *Rn* (Fig. 3a) because of the decrease in *P* is favorable condition for the increase in *Rn*, which can result in positive influences of *Rn* on the surface dryness trend. We anticipate that aerosols can play an important role in the decrease in *Rn* in the arid region by absorbing and scattering solar irradiance. Furthermore, additional heating due to urbanization may cause different trends in atmospheric water demands between urban and rural areas (Han et al., 2012; Ren and Zhou, 2014). However, examining the effects of LULCC and aerosols on trends in surface dryness lies beyond scope of the present study.

The effects of *Ta* and *RH*, which act to dry land surfaces, increased significantly in recent decades in all regions (Figs. 6 and 7). Moreover, over the humid monsoon region, increases in *RH* show a greater influence on trends in surface dryness than increases in *P*. This is an unusual situation considering the large variability of summer monsoon rainfall over continental East Asia. The large influence of *RH* is supported by steep warming over the humid monsoon area after the early 1980s. This kind of drying mechanism is consistent with that suggested in assessments dealing with changes in surface dryness during the 20th and 21st centuries using reconstructed data and future climate projections (Sherwood and Fu, 2014). Thus, our study could be an observed precursor of the projected drying trends over the humid areas in 21st century (Cook et al., 2014; Yin et al., 2015). The present results also indicate that drying of the land surface in response to warming is already in progress, not simply a future risk. Therefore, water management planning must consider the increased water demands associated with warming in order to mitigate water scarcity, even in the wet monsoon regions.

Code and data availability

Codes of NCAR Command Language version 6.3.0, Python, and Interactive Data Language for calculation and climate data are available upon request to the correspondence author Su-Jong Jeong (waterbell@gmail.com).

Author Contributions

C.-E. P. conceived and designed the study, analysed data, and wrote the paper. S.-J. J. helped conceive of the study, and wrote the paper. C.-H. H. wrote the paper. H. P. analysed data, and wrote the paper. S. P., J. K., and S. F. helped conceive of the study and wrote the paper.

Competing interests

The authors declare no competing financial interest.

Acknowledgements

This study was funded by the Korea Ministry of Environment as the “Climate Change Correspondence Program”.

References

Allen, R. G., Pereira, L. S., Raes, D., and Smith, M.: Crop evapotranspiration–guidelines for computing crop water requirements–FAO Irrigation and drainage Paper 56, FAO, 1998.

Beaulieu, C., Chen, J., and Sarmiento, J. L.: Change-point analysis as a tool to detect abrupt climate variations, Phil. Trans. R. Soc. A., 370, 1228-1249, doi:10.1098/rsta.2011.0383, 2012.

Chattopadhyay, N., Hulme, M.: Evaporation and potential evapotranspiration in India under conditions of recent and future climate change, Agric. Forest Meteorol., 87, 55-73, 1997.

Cook, B. I., Smerdon, J. E., Seager, R., and Coats, S.: Global warming and 21st century drying, Clim. Dyn., 43, 2607–2627, doi:10.1007/s00382-014-2075-y, 2014.

Dai, A.: Increasing drought under global warming in observations and models, Nature Clim. Change. 3, 52–28, doi:10.1038/nclimate1633, 2013.

Ding, Y., Wang Z., and Sun Y.: Inter-decadal variation of the summer precipitation in East China and its association with decreasing Asian summer monsoon. Part I: Observed evidences, Int. J. Climatol., 28, 1139–1161, doi:10.1002/joc.1615 2008.

Dinpashoh, Y., Jhajharia, D., Fakheri-Fard, A., Singh, V. P., and Kahya, E.: Trends in reference crop evapotranspiration over Iran, J. Hydrology, 399, 422-423, doi:10.1016/j.jhydrol.2011.01.021, 2011.

Estes, L. D., Chaney, N. W., Herrera-Estrada, J., Sheffield, J., Caylor, K. K., and Wood, E. F.: Changing water availability during the African maize-growing season, 1979-2010, Environ. Res. Lett., 9, doi:10.1088/1748-9326/9/7/075005, 2014.

Feng, S. and Fu, Q.: Expansion of global drylands under a warming climate, Atmos. Chem. Phys., 13, 10081–10094, doi:10.5194/acp-13-10081-2013, 2013.

Fu, Q. and Feng, S.: Responses of terrestrial aridity to global warming, J. Geophys. Res. Atmos., 119, doi:10.1002/2014JD021608, 2014.

Ge, Q., Wang, F., and Luterbacher, J.: Improved estimation of average warming trend of China from 1951–2010 based on satellite observed land-use data, Clim. Change, 121, 365–379, doi:10.1007/s10584-013-0867-4, 2013.

Geng, Q. L., Wu, P, Zhang, Q., Zhao, X., and Wang, Y.: Dry/wet climate zoning and delimitation of arid areas of Northwest China based on a data-driven fashion, J. Arid. Land., 6, 287–299, doi:10.1007/s40333-013-0206-7, 2014.

Gong, D.-Y. and Ho, C.-H.: Shift in the summer rainfall over the Yangtze River valley in the late 1970s, Geophys. Res. Lett., 29, 78-1, doi:10.1029/2001GL014523, 2002.

Greve. P., Orlowsky, B., Mueller, B., Sheffield, J., Reichstein, M., and Seneviratne, S. I.: Global assessment of trends in wetting and drying over land, Nature Geosci., 7, 716–721, doi:10.1038/ngeo2247, 2014.

Guo, L., Highwood, E. J., Shaffrey, L. C., and Turner, A. G.: The effect of regional changes in anthropogenic aerosols on rainfall of the East Asian Summer Monsoon, Atmos. Chem. Phys., 13, 1521-1534, doi:10.5194/acp-13-1521-2013 2013.

Ha, K.-J., Heo, K.-Y., Lee, S.-S., Yun, K.-S., and Jhun, J.-G.: Variability in the East Asian Monsoon: a review, Met. Apps., 19, 200-215, doi:10.1002/met.1320, 2012.

Han, S., Xu, D., and Wang, S.: Decreasing potential evaporation trends in China from 1956 to 2005: Accelerated in regions with significant agricultural influence?, Agric. Forest Meteorol., 154-155, 44–56, doi:10.1016/j.agrformet.2011.10.009, 2012.

Hegerl, G. C., Black, E., Allan, R. P., Ingram, W. J., Polson, D., Trenberth, K. E., Chadwick, R. S., Arkin, P. A., Sarojini, B. B., Becker, A., Dai, A., Durack, P. J., Easterling, D., Fowler, H. J., Kendon, E. J., Huffman, G. J., Liu, C., Marsh, R., New, M., Osborn, T. J., Skliris, N., Stott, P. A., Vidale, P.-L., Wijffels, S. E., Wilcox, L. J., Willett, K. M., and Zhang, X.: Challenges in quantifying changes in the global water cycle, Bull. Amer. Meteor. Soc., 96, 1097–1115, doi:10.1175/BAMS-D-13-00212.1, 2015.

Huang, H., Han, Y., Cao, M., Song, J., and Xiao, H.: Spatial-Temporal Variation of Aridity Index of China during 1960-2013, Adv. in Meteorol., doi:10.1155/2016/1536135, 2016.

Huang, J., Yu, H., Guan, X., Wang, G., and Guo, R.: Accelerated dryland expansion under climate change, Nature. Clim. Change, 6, 166-171, doi:10.1038/nclimate2837, 2016.

Jeong, S.-J., Ho, C.-H., Piao, S., Kim, J., Ciais, P., Lee, Y.-B., Jhun, J.-G., and Park, S.-K.: Effects of double cropping on summer climate of the North China Plain and neighbouring regions, Nature Clim. Change, 4, 615-619, doi:10.1038/nclimate2266, 2014.

Kitoh, A., Endo, H., Krishna, K. K., Cavalcanti, I. F. A., Goswami, P., and Zhou, T.: Monsoons in a changing world: A regional perspective in a global context, J. Geophys. Res. Atmos., 118, 3053–3065, doi:10.1002/jgrd.50258, 2013.

Liu, C. and Allan, R. P.: Observed and simulated precipitation responses in wet and dry regions 1850-2100, Environ. Res. Lett., 8, doi:10.1088/1748-9326/8/3/034002, 2013.

Liu. H. W., Zhou, T. J., Zhu, Y. X., and Lin, Y. H.: The strengthening East Asia summer monsoon since the early 1990s, Chinese Sci. Bull., 57, 1553–1558, doi:10.1007/s11434-012-4991-8, 2012.

Liu, M., Shen, Y., Zeng, Y., and Liu, C.: Trends of pan evaporation in China in recent 50 years in China. J. Geogr. Sci., 20, 557–568, 2010.

Lund, R., Reeves, J.: Detection of undocumented changepoints: A revision of the two-phase regression model, J. Clim., 2547-2554, 2002.

Menon, S., Hansen J., Nazarenko L., and Luo Y.: Climate Effects of Black Carbon Aerosols in China and India, Science, 297, 2250-2253, doi:10.1126/science.1075159, 2002.

Park Williams, A., Allen, C. D., Macalady, A. K., Griffin, D., Woodhouse, C. A., Meko, D. M., Swetnam, T. W., Rauscher, S. A., Seager, R., Grissino-Mayer, H. D., Dean, J. S., Cook, E. R., Gangodagamage, C., Cai, M., and McDowell, N. G.: Temperature as a potent driver of regional forest drought stress and tree mortality, Nature Clim. Change, 3, 292–297, doi:10.1038/nclimate1693, 2013.

Pettitt, A. N.: A simple cumulative sum type statistic for the change-point problem with zero-one observation, Biometrika, 67, 1, 79–84, 1980.

Piao, S., Ciais, P., Huang, Y., Shen, Z., Peng, S., Li, J., Zhou, L., Liu, H., Ma, Y., Ding, Y., Friedlingstein, P., Liu, C., Tan, K., Yu, Y., Zhang, T., and Fang, J.: The impacts of climate change on water resources and agriculture in China, Nature, 467, 43–51, doi:10.1038/nature09364, 2010.

Ren G. and Zhou Y.: Urbanization Effect on Trends of Extreme Temperature Indices of National Stations over Mainland China, 1961–2008, J. Clim., 27, 2340-2360, doi10.1175/JCLI-D-13-00393.1, 2014.

Roxy, M. K., Ritika, K., Terray, P., Murtugudde, R., Ashok, K., and Goswami, B.N.: Drying of Indian subcontinent by rapid Indian Ocean warming and a weakening land-sea thermal gradient, Nat. Commun., 6, doi:10.1038/ncomms8423, 2015.

Shan, N., Shi, Z., Yang, X., Zhang, X, Guo, H, Zhang, B., and Zhang, Z.: Trends in potential evapotranspiration from 1960 to 2013 for a desertification-prone region of China, Int. J. Climatol., 10, 3434-3445, doi:10.1002/joc.4566, 2015.

Sherwood, S. and Fu, Q.: A drier future?, Science, 343, 737–739, doi:10.1126/science.1247620, 2014.

Shi, Y., Shen, Y., Kang, E., Li, D., Ding, Y., Zhang, G., and Hu, R.: Recent and Future Climate Change in Northwest China, Climatic Change, 80, 379-393, doi:10.1007/s10584-006-9121-7, 2007.

Tang, W.-J., Yang, K., Qin, J., Cheng, C. C. K., and He, J.: Solar radiation trend across China in recent decades: A revisit with quality-controlled data, Atmos. Chem. Phys., 11, 393–406, doi:10.5194/acp-11-393-2011, 2011.

UNEP: World atlas of desertification, edited by Middleton, N., Thomas, D. S. G., Edward Arnold, London, 1992.

Wang, B. and Ding, Q.: Changes in global monsoon precipitation over the past 56 years, Geophys. Res. Lett., 33, L06711, doi:10.1029/2005GL025347, 2006.

Wang, B., Liu, J., Kim, H.-J., Webster, P. J., and Yim, S.-Y. Recent change of the global monsoon precipitation (1979–2008), Clim. Dyn., 39, 1123–1135, doi:10.1007/s00382-011-1266-z, 2012.

Westerling, A. L., Hidalgo, H. G., Cayan, D. R., and Swetnam, T. W.: Warming and earlier spring increase western U.S. forest wildfire activity, Science, 313, 940–943, doi:10.1126/science.1128834, 2006.

Wu, S., Yin. Y., Zheng, D., and Yang, Q.: Moisture conditions and climate trends in China during the period 1971–2000, Int. J. Climatol., 26, 193-206, doi:10.1002/joc.1245, 2006.

Yin, Y., Wu, S., Chen, G., and Dai, E.: Attribution analyses of potential evapotranspiration changes in China since the 1960s, Theor. Appl. Climatol., 101, 19-28, doi:10.1007/s00704-009-0197-7, 2010.

Yin, Y., Ma, D., Wu, S., and Pan, T.: Projections of aridity and its regional variability over China in the mid-21st century, Int. J. Climatol., 14, 4387-4398, doi:10.1002/joc.4295, 2015.

Yue, T.-X., Zhao, N., Ramsey, R. D., Wang, C.-L., Fan, Z.-Meng, Chen, C.-F., Lu, Y.-M., and Li, B.-L.: Climate change trend in China, with improved accuracy, Clim. Change, 120, 137–151, doi:10.1007/s10584-013-0785-5, 2013.

Zhai, P. M., Zhang, X. B., Wan, H., and Pan, X. H.: Trends in total precipitation and frequency of daily precipitation extremes over China, J. Clim. 18, 1096–1108, doi:10.1175/JCLI-3318.1, 2005.

Zhang, Q., Xu, C.-Y., and Zhang, Z.-X.: Observed changes of drought/wetness episodes in the Pearl River basin, China, using the standardized precipitation index and aridity index, Theor. Appl. Climatol., 98, 89-99, doi:10.1007/s00704-008-0095-4, 2009.

Zhou, T., Zhang, L., and Li, H.: Changes in global land monsoon area and total rainfall accumulation over the last half century, Geophys. Res. Lett., 35, L16707, doi:10.1029/2008GL034881, 2008.

Zhu, C., Wang, B., Qian, W., and Zhang, B.: Recent weakening of northern East Asian summer monsoon: A possible response to global warming, Geophys. Res. Lett.,39, doi:10.1029/2012GL051155, 2012.

Figures

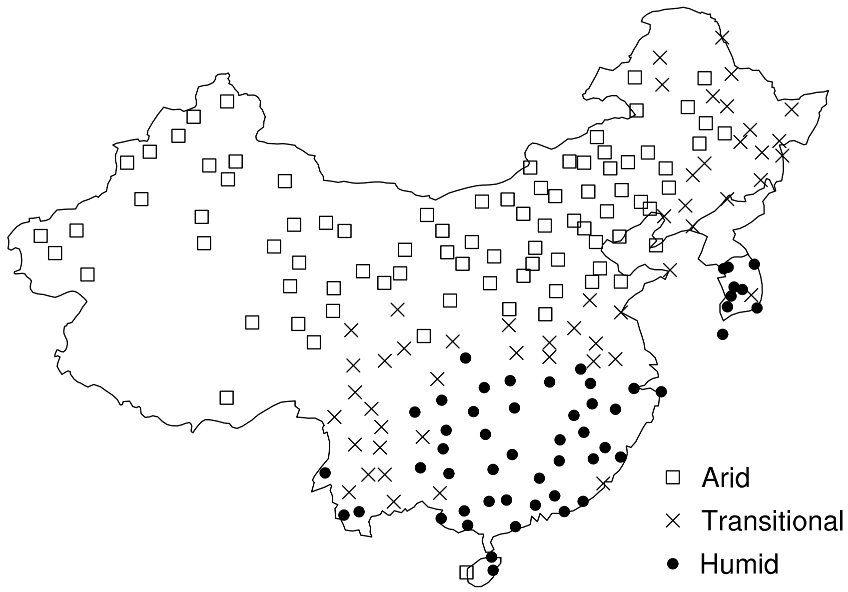

Figure 1. Spatial distribution of 189 meteorological stations in analysis domain. Spatial locations of 179 and 10 meteorological sites of Mainland China and South Korea. Empty squares, crosses and filled circles indicate stations that classified by arid, transitional, and humid regimes based on 50-year climatological *PET/P* for the period of 1961-2010.

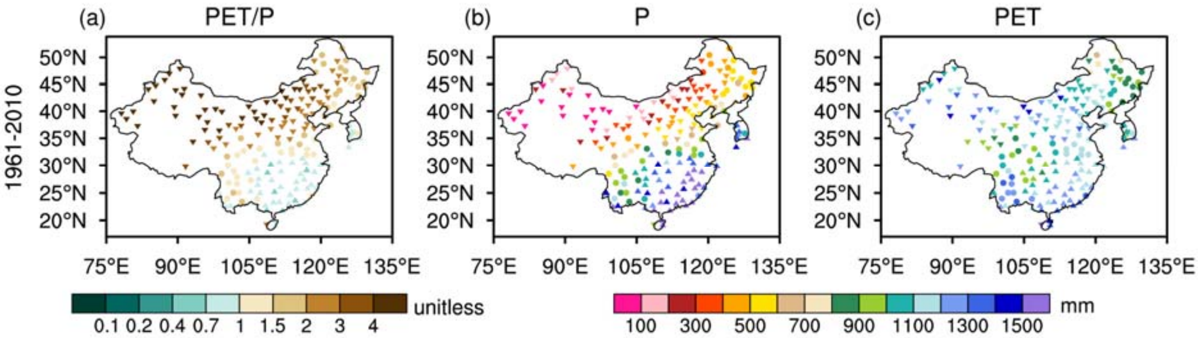

Figure 2. Spatial distributions of the climatologies of *PET/P* (a), *P* (b), and *PET* (c) over continental East Asia for the period of 1961-2010. Inverse triangles, circles, and triangles represent stations classified as arid, transitional, and humid regions, respectively.

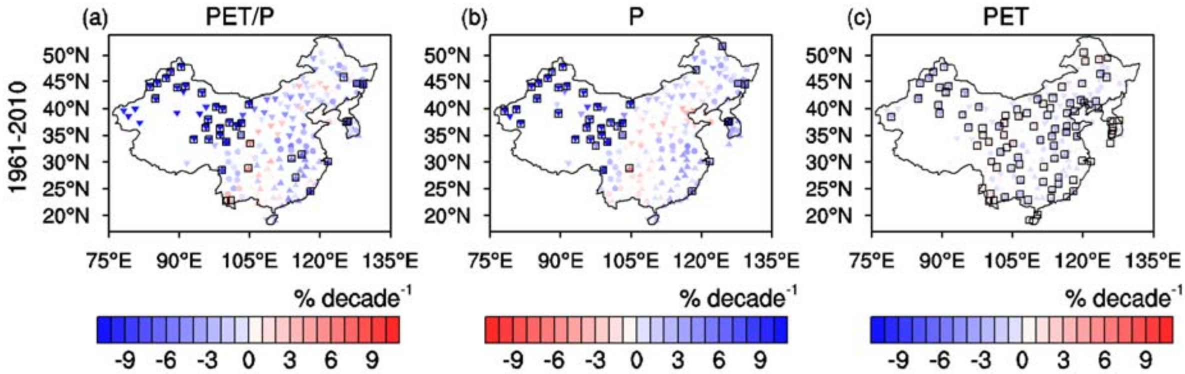

Figure 3. Spatial distributions of the trends in *PET/P*, *P*, and *PET* over continental East Asia. a−c: The spatial distribution of trends in the annual-mean *PET/P* (a), *P* (b), and *PET* (c) for the period of 1961−2010. Inverse triangles, circles, and triangles represent stations classified as arid, transitional, and humid regions, respectively. The open squares indicate that the trend is significant at the 95% confidence level.

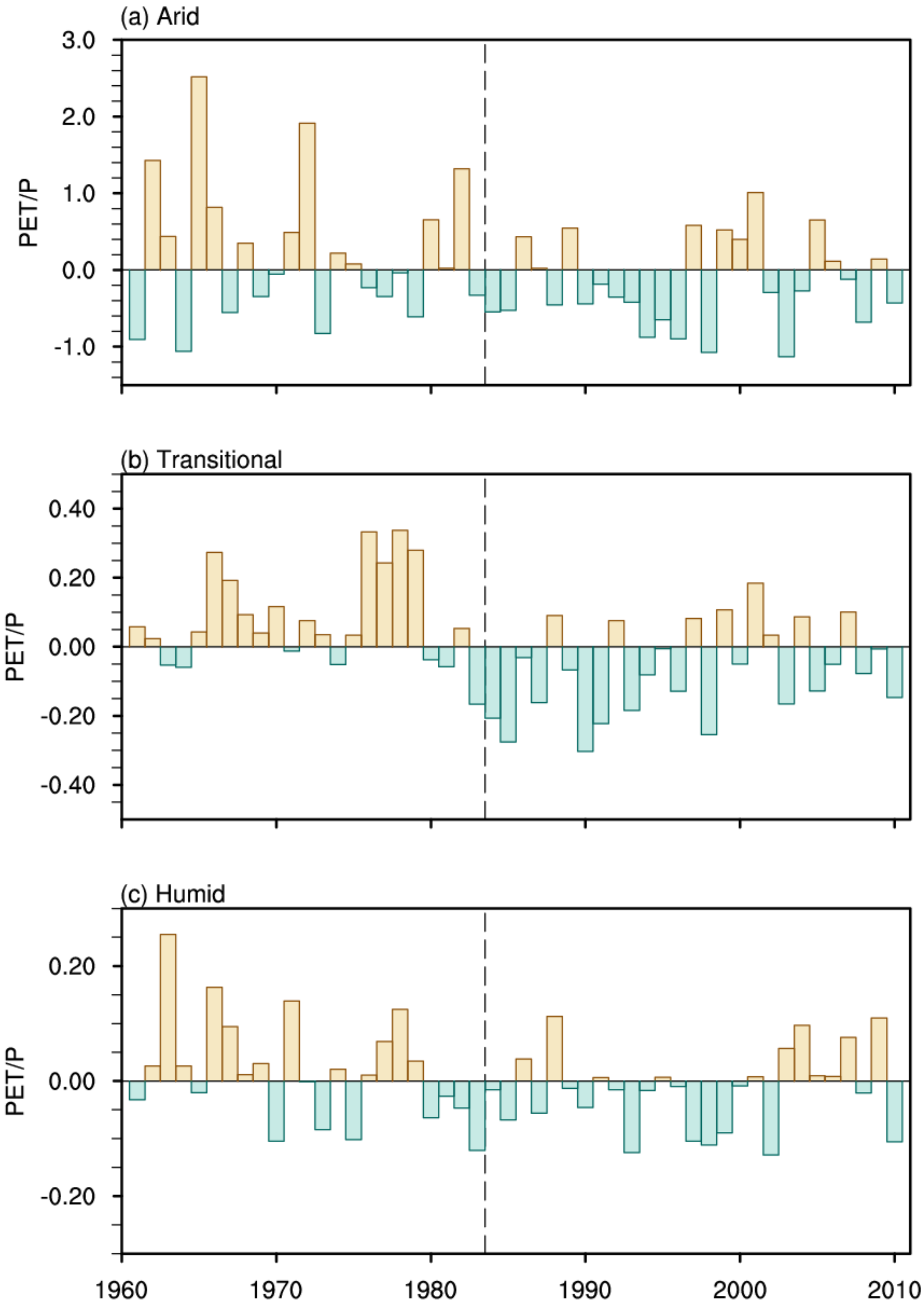

Figure 4. Interannual variations of the annual-mean *PET/P* over the (a) arid, (b) transitional, and (c) humid regions located to the east of 100ºE. Yellow and blue bars indicate the positive and negative anomalies for *PET/P*, respectively.

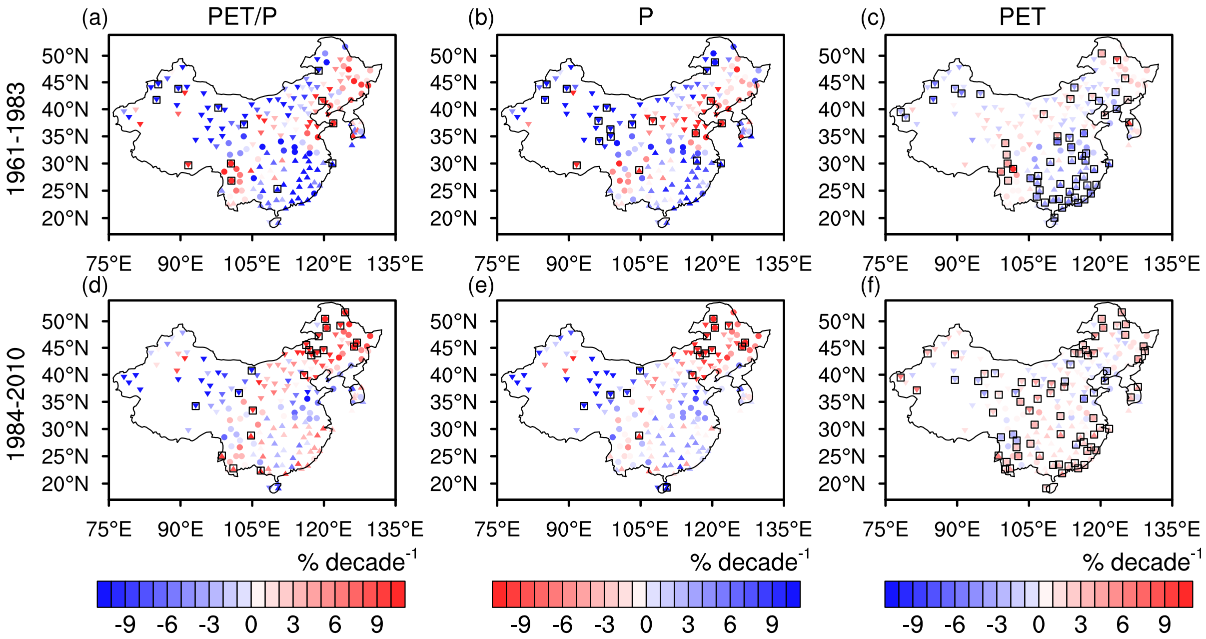

Figure 5: Spatial distributions of the trends in *PET/P*, *P*, and *PET* over continental East Asia. a−c: The spatial distribution of trends in the annual-mean *PET/P* (a), *P* (b), and *PET* (c) for the period of 1961−1983. d−f: as a−c, but for the period 1984−2010. Inverse triangles, circles, and triangles represent stations classified as arid, transitional, and humid regions, respectively. The open squares indicate that the trend is significant at the 95% confidence level.

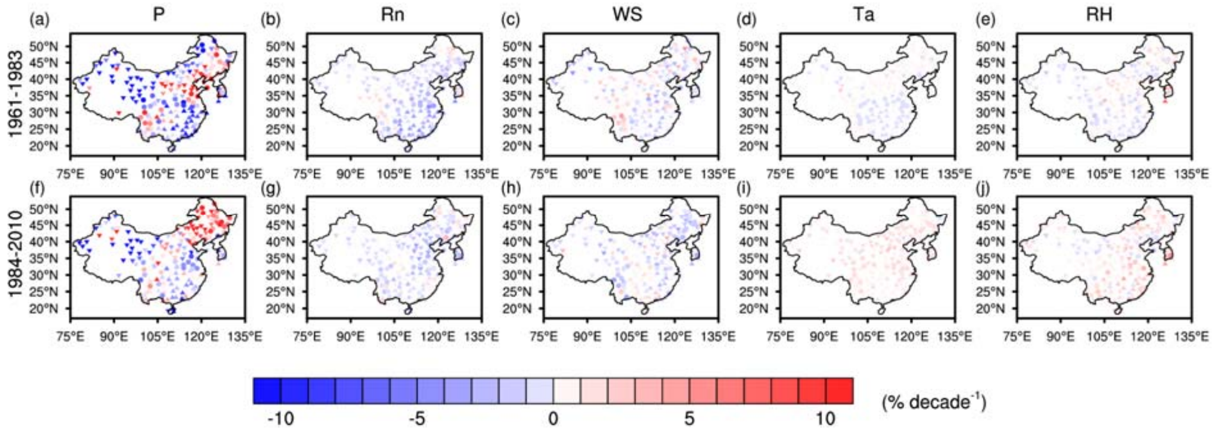

Figure 6. Spatial distributions of the relative influences of five climate parameters on the *PET/P* trends. a-e, The spatial distribution of relative influences of the changes in *P* (a), *Rn* (b), *WS* (c), *Ta* (d), and *RH* (e) on the *PET/P* trends for the period of 1961-1983. f-j, as a-e, but for the period of 1984-2010. Inverse triangles, circles, and triangles represent stations classified as arid, transitional, and humid regions, respectively.

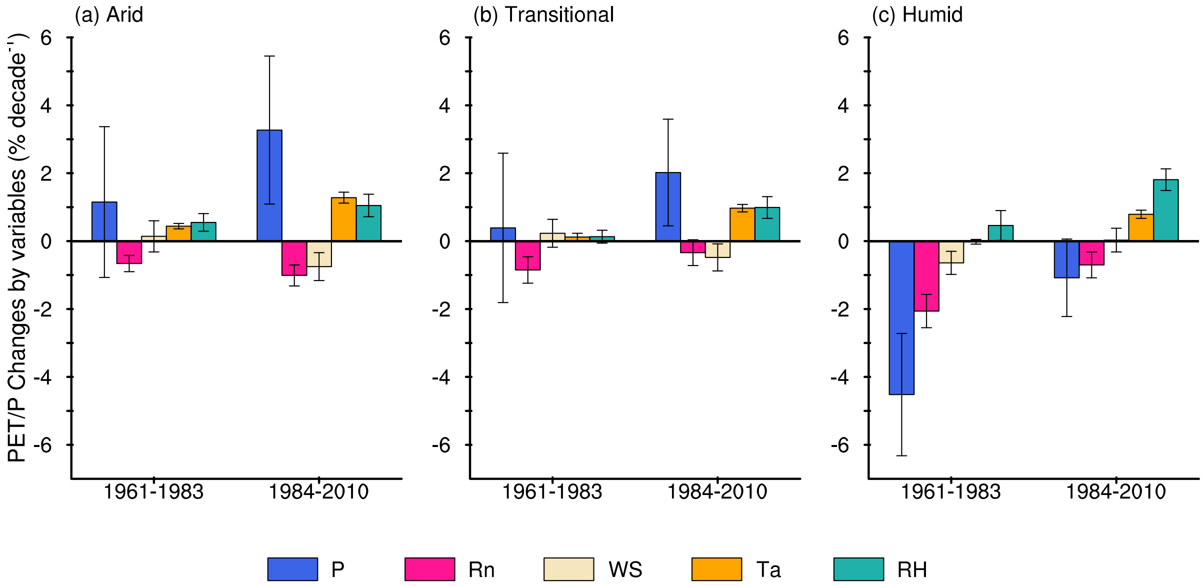

Figure 7: Relative influences (% decade^{-1}) of five climate parameters averaged over the three hydro-climate regimes: arid (a), transitional (b), and humid (c). The influences are computed for the two analysis periods: 1961−1983 and 1984−2010. Blue, pink, beige, orange, and cyan bars represent the respective influences of *P*, *Rn*, *WS*, *Ta*, and *RH*. Error bars represent confidence intervals at the 95% confidence level.

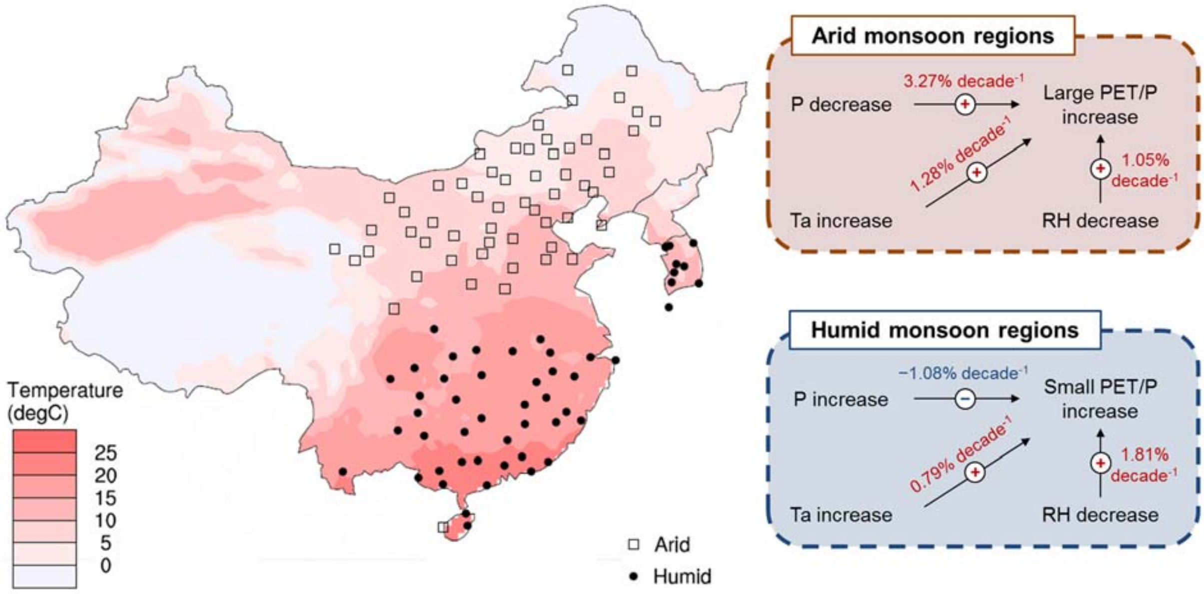

Figure 8: Schematic diagram of the contributions of *P*, *Ta*, and *RH* on the *PET/P* trends in arid and humid monsoon regions for the period of 1983−2010. Diagrams of the influences of *P*, *Ta*, and *RH* on the trend in *PET/P* over arid and humid monsoon regions in 1983−2010 are located to the right of annual-mean temperature over continental East Asia for 1961−2010 (°C). Empty squares and filled circles are stations classified as arid and humid monsoon regions (east of 100°E), respectively.